Nanoscale

RSC Publishing

PAPER

Surface chemistry of gold nanorods: origin of cell membrane damage and cytotoxicity

Cite this: *Nanoscale*, 2013, **5**, 8384

Liming Wang,†[a] Xiumei Jiang,†[a] Yinglu Ji,[b] Ru Bai,[a] Yuliang Zhao,[a] Xiaochun Wu*[b] and Chunying Chen*[a]

Received 1st April 2013
Accepted 30th May 2013

DOI: 10.1039/c3nr01626a

www.rsc.org/nanoscale

We investigated how surface chemistry influences the interaction between gold nanorods (AuNRs) and cell membranes and the subsequent cytotoxicity arising from them in a serum-free cell culture system. Our results showed that the AuNRs coated with cetyl trimethylammonium bromide (CTAB) molecules can generate defects in the cell membrane and induce cell death, mainly due to the unique bilayer structure of CTAB molecules on the surface of the rods rather than their charge. Compared to CTAB-capped nanorods, positively charged polyelectrolyte-coated, *i.e.* poly(diallyldimethyl ammonium chloride) (PDDAC), AuNRs show improved biocompatibility towards cells. Thus, the present results indicate that the nature of surface molecules, especially their packing structures on the surface of AuNRs rather than surface charge, play a more crucial role in determining cytotoxicity. These findings about interfacial interactions could also explain the effects of internalized AuNRs on the structures or functions of organelles. This study will help understanding of the toxic nature of AuNRs and guide rational design of the surface chemistry of AuNRs for good biocompatibility in pharmaceutical therapy.

Introduction

As a super star in the field of nanotechnology, gold nanorods (AuNRs) with unique physicochemical properties, have attracted more and more attention due to their promising applications in biomedicine.[1–6] It thus becomes increasingly important to understand the biological effects of AuNRs in order to expand our knowledge about what happens at bio–nano interfaces.[1,7,8] New knowledge is necessary not only for safe application and risk prediction but also for rational design of multifunctional and responsive nanocarriers based on AuNRs.[9–13]

Aspect ratio, size and surface chemistry are three basic properties to consider when evaluating the biological effects of AuNRs.[14–16] It has been reported that the above properties of AuNRs determine many biological responses for example, protein adsorption,[16] blood circulation, *in vivo* biodistribution,[17–19] cell uptake and removal,[15,16] and cytotoxicity,[15,16] *etc*. Among these studies, surface chemistry is considered to be the major factor mediating the cytotoxicity of AuNRs. Cetyl trimethylammonium bromide (CTAB) is widely used to control the growth of rods and maintain their good dispersibility in an aqueous phase during the preparation of AuNRs. CTAB is a cationic surfactant that forms a bilayer structure on the surface of AuNRs.[20] Previous studies have indicated that CTAB-coated AuNRs (CTAB–AuNRs) are toxic to many types of cells, while additional coatings of polystyrene sulfonate (PSS) or poly (diallyldimethyl ammonium chloride) (PDDAC) *via* electrostatic interactions, or replacement by thiol functionalized carboxy poly(ethylene glycol) (HS-PEG-COOH) can reduce the cytotoxicity.[15–18,21] A series of studies indicated that both released CTAB in the solution and CTAB in a bilayer on AuNRs contributed to the toxicity of CTAB–AuNRs.[11,15,22] As a cationic surfactant, CTAB itself can diffuse across a cell membrane directly and targets mitochondria causing apoptosis.[23] On the other hand, a CTAB bilayer can be internalized and translocated along with AuNRs,[11] which is different from dissolved CTAB molecules or CTAB micelles. From this point of view, the interfacial interaction of a cell membrane with CTAB–AuNRs should be more related to the nature of their toxicity. However, the key detailed structural evidence about the interaction mode of AuNRs with cell membranes is still lacking.

In the present work, we aimed to study how the surface chemistry of AuNRs influences their interaction with cell membrane and induced cytotoxicity. Four types of AuNRs, including positively charged CTAB and PDDAC coated rods, and negatively charged PSS and HS-PEG-COOH coated rods were used to study the surface effects of AuNRs on lung cancer epithelial cells (A549). In a serum-free cell culture system, cell viability, the integrity of the cell membrane, and detailed interfacial structures of the cell membrane and organelles were

[a]*CAS Key Laboratory for Biomedical Effects of Nanomaterials and Nanosafety, Institute of High Energy Physics and National Center for Nanoscience and Technology, Beijing, China. E-mail: chenchy@nanoctr.cn*

[b]*CAS Key Laboratory of Standardization and Measurement for Nanotechnology, National Center for Nanoscience and Technology, Beijing, China. E-mail: wuxc@nanoctr.cn*

† These authors contributed equally to this work.

evaluated in order to understand the toxicity mechanism. The interaction of AuNRs with membrane structures can also be employed to explain why different surface chemistry causes distinct effects on cell viability, lysosomal membrane permeation and mitochondrial membrane potential in complete cell culture media with serum.

Results and discussion

Characterization of AuNRs

CTAB–AuNRs were prepared according to reports in previous publications.[16,24] Mean sizes were obtained by measuring 100 nanorods using a transmission electron microscope (TEM). The rods have a mean aspect ratio of 4.2 with a mean length of 55.6 ± 7.8 nm and width of 13.3 ± 1.8 nm (Fig. 1a). Based on CTAB–AuNRs, electrostatic adsorption of PSS and PDDAC produced the PSS–AuNRs and PDDAC–AuNRs, respectively. Direct ligand replacement of CTAB molecules on the AuNRs with HS-PEG-COOH molecules formed PEG–AuNRs. These AuNRs have similar UV-vis-NIR spectra with a longitudinal surface plasmon resonance peak at approximately 810 nm, which means that these AuNRs are well dispersed in water after surface modification (Fig. 1c). The surface charge of the AuNRs is expressed by the zeta potential. CTAB–AuNRs and PDDAC–AuNRs have positive surface charge, while PSS–AuNRs and PEG–AuNRs have negative surface charge (Fig. 1d). The surface charge of PDDAC–AuNRs is much higher than that of CTAB-coated rods. The zeta potentials of all the AuNRs are greater than 20 mV, which suggests good stability in the solution.

Cytotoxicity evaluation of AuNRs

In order to understand whether the toxicity of AuNRs depends on surface chemistry, two systems, serum-free medium and complete medium with 10% fetal bovine serum (FBS), were used. In serum-free medium, the viability of the A549 cells decreased to about 60% at 12 h and 40% at 24 h when exposed to 50 μM CTAB–AuNRs, while other surface coated AuNRs caused much less toxicity (Fig. 2a). In order to establish the origin of the toxicity, we measured the toxicity of the supernatant of CTAB–AuNRs, in which free CTAB molecules were dissolved. The supernatant was obtained by centrifuging the CTAB–AuNR suspension. Results showed that the supernatant is much less toxic than the CTAB–AuNRs, which indicated that the toxicity of CTAB–AuNRs mainly comes from the CTAB–AuNRs themselves rather than free CTAB, which is supported by previous work.[11] As mentioned above, PDDAC–AuNRs have a much higher positive charge than CTAB–AuNRs; however, they had a negligible effect on cell viability. It is thus suggested that other surface properties rather than surface charge play the most important role in inducing toxicity and a detailed investigation into the interfacial interaction of the AuNR surface with cells may reveal the possible reason.

To detect cell membrane injury, the release of lactic acid dehydrogenase (LDH) from the cytoplasm, a well known biochemical indicator of cell membrane integrity, was measured. It has been used to evaluate the interaction between nanoparticles and membranes.[25] For healthy cells, LDH is mainly located in the cytoplasm and its extracellular release indicates increased permeation of the cytoplasm membrane or damage to the cell membrane. According to the result of the LDH assay, we observed that CTAB–AuNRs induced more LDH release, in a time and concentration dependent manner, than other AuNRs and the CTAB supernatant (Fig. 2b). Furthermore, the greater damage to the cell membrane caused by CTAB–AuNRs changed the structure of the cell membranes and induced subsequent cell death, which was supported by the Live–Dead assay (Fig. 2c).

Therefore, we concluded that the surface properties of CTAB–AuNRs mediate the nature of their toxicity and more detailed information about the interfacial interaction between the CTAB surface and cell membrane will be helpful to uncover the possible mechanism.

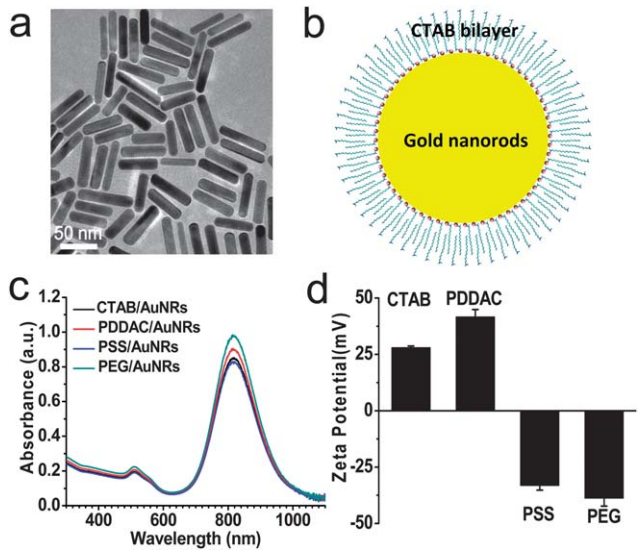

Fig. 1 Characterization of AuNRs. (a) TEM image of CTAB-coated AuNRs. (b) Cartoon of the CTAB bilayer assembled on the surface of AuNRs from the section view. (c) UV-vis-NIR absorption spectra and (d) mean zeta potentials of CTAB–AuNRs, PDDAC–AuNRs, PSS–AuNRs and PEG-modified AuNRs.

Interaction between AuNRs and the cell membrane

The cell membrane is mainly composed of a phospholipid bilayer and proteins with negative charges, which probably drives the electrostatic adsorption of positive charged AuNRs onto the cell membrane. Once AuNRs contact the cell membrane, they can be recognized by cells and trigger a series of responses *i.e.* uptake, translocation, accumulation, exclusion and cell death.[11,14,16] The type of contact and the state of the AuNRs on the cell membrane may affect the cell responses, which is critical in understanding their toxic nature.

In order to establish the surface effect of the AuNRs, electron microscopes were used to study how AuNRs with different coatings influence the structure of the cell membrane. In a serum-free culture medium, untreated cells have an intact membrane surface covered with plenty of long microvilli, according to ESEM (Fig. 3a and f). By incubating the cells with

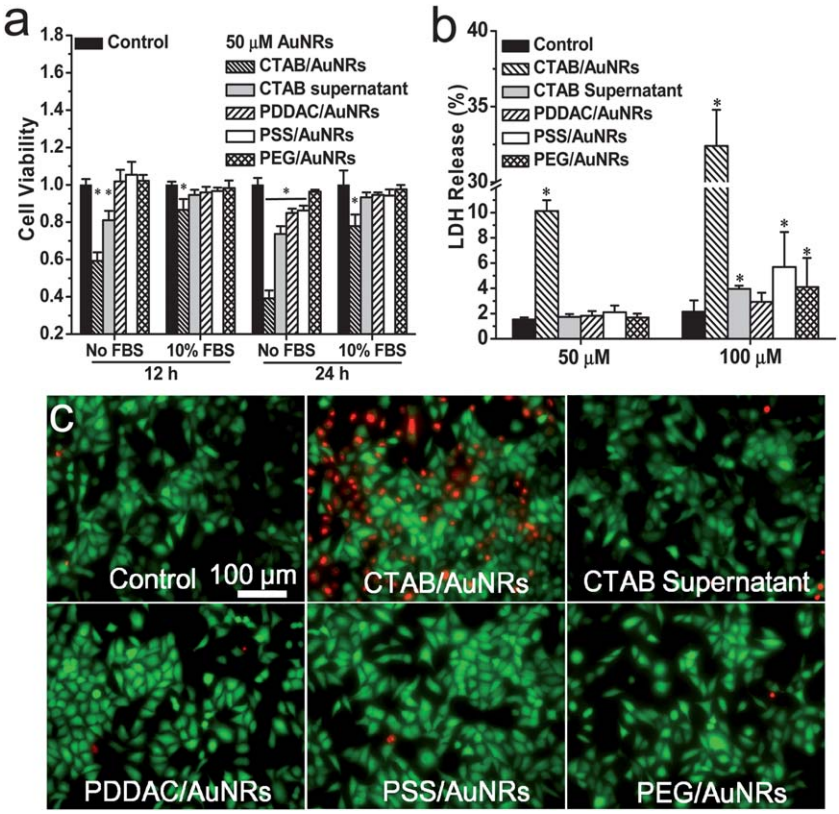

Fig. 2 The influence of the surface properties of AuNRs on A549 cells. (a) In a serum-free medium or complete medium with 10% FBS, the surface effects of 50 μM AuNRs on A549 cell viability according to a CCK-8 assay. (b) In a serum-free medium, cytotoxicity evaluation of 50 μM AuNRs and CTAB supernatant from CTAB–AuNRs solution by LDH release and (c) live–dead assay after 24 h exposure. * Indicates significant effects of AuNRs on cells ($p < 0.05$). Results are reported as mean values and standard deviations, $N = 3$.

four types of AuNRs for 12 h, both the state of the AuNRs and their effect on the membrane structures were distinguished. CTAB–AuNRs aggregated on the cell membrane and most of the long microvilli disappeared. Some large blebs appeared around the AuNRs and some defects could be found in the blebs or on the membrane (Fig. 3b and g). The defective structure was indicated by white arrowheads (Fig. 3g). In contrast, very few PDDAC–AuNRs aggregated on the membrane and the number of long microvilli decreased somewhat (Fig. 3c and h). However, neither blebs nor obvious defects were observed on the membrane for PDDAC–AuNR exposed cells. Except for many long microvilli on the membrane, a similar phenomenon was observed for PSS–AuNRs and PEG–AuNRs (Fig. 3d, e, i and j). The ESEM results clearly demonstrated that surface molecules

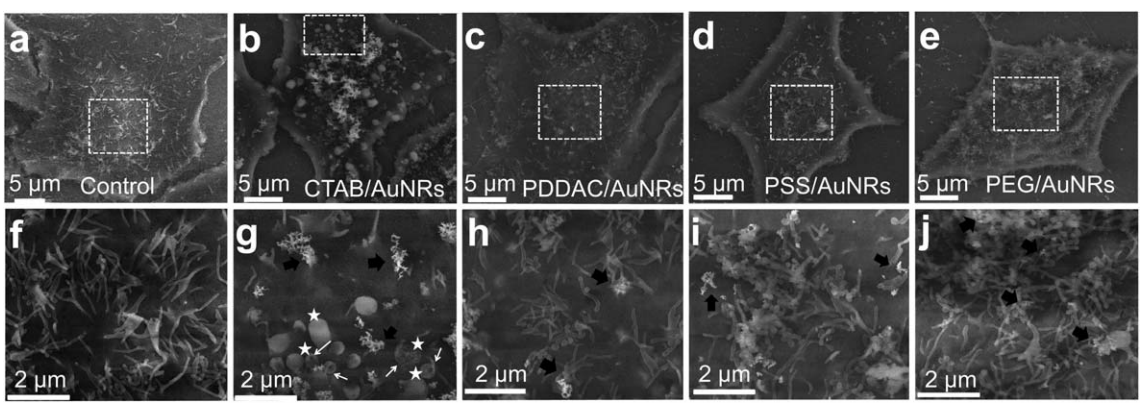

Fig. 3 ESEM images for cytoplasm membrane structures. In serum-free medium, untreated A549 cells (a and f); A549 cells exposed to 50 μM AuNRs with four kinds of surface coating, CTAB (b and g), PDDAC (c and h), PSS (d and i) and HS-PEG-COOH (e and j) for 12 h, respectively. The upper figures (a–e) represent a whole cell image and their magnified images are shown below (f–j). In (g–j) the black arrowheads, white stars and white arrowheads indicate AuNR aggregates, blebs and induced defects in the membranes, respectively.

rather than surface charges are responsible for the cell membrane injury, as a positively charged coating on the AuNRs, like PDDAC, did not induce serious membrane damage such as the disappearance of microvilli and the formation of holes in the membrane.

The TEM images also clearly showed the changes in membrane structure after treatment with CTAB–AuNRs. We observed some aggregates of AuNRs on the cell membrane and some CTAB–AuNRs inserted and penetrated into the cell membrane (Fig. 4b and g). This process may induce the formation of defects as supported by ESEM images and subsequent LDH release, suggesting injury to the cell membrane. Fewer CTAB–AuNRs were located within the cells than PDDAC (Fig. 4c and h) and PSS-coated rods (Fig. 4d and i). This is due to easier attachment of CTAB–AuNRs on the membrane and formation of larger AuNR aggregates, both suppress internalization by endocytosis. While PDDAC and PSS-coated AuNRs, with very few aggregates on the cell membrane, were internalized into the cells and induced formation of more endosomes or lysosomes compared to control cells. In addition, the structure of the mitochondria did not change obviously for these two AuNRs, while swollen mitochondria appeared after treatment with CTAB–AuNRs. To our surprise, very few PEG–AuNRs were observed around the cell membrane and internalized in the cells (Fig. 4e and j). The possible reason is that the negatively charged carboxyl groups orientated towards the aqueous environment prevent PEG–AuNRs from getting close to the cell membrane.

Interaction between AuNRs and organelles

In physiological fluids, the surface of the AuNRs can easily adsorb multiple types of proteins to form a protein corona. It is hard for AuNRs to expose their surface to the cell membrane directly. In a complete cell culture medium, protein-adsorbed AuNRs can be easily internalized and transported from endosomes to lysosomes. In an acidic environment, the protein corona prefers to detach from the surface of the AuNRs due to easy denaturing and subsequent hydrolysis by enzymes.[11] In that case, the surface of the AuNRs is exposed and could interact with the membrane structure directly. Acridine orange (AO) staining was used to study the integrity of the lysosomal membrane because it can selectively accumulate in acidic organelles and emit red fluorescence but decreases this fluorescence when the local pH rises. Intracellular CTAB–AuNRs increased lysosomal membrane permeation (LMP) as shown by weakened red fluorescence and enhanced green fluorescence (Fig. 5a). The changes in lysosomal membrane integrity could also be observed by TEM (Fig. 5b and c). Increased LMP leads to the release of digestive enzymes into the cytoplasm and triggers mitochondrion-mediated apoptosis.[26] Moreover, released CTAB–AuNRs were found to target mitochondria. These two factors contributed to a decreased mitochondrial membrane potential (MMP) determined by Rhodamine 123 (Fig. 5d) and subsequent decreased cell viability (Fig. 2a). The lowered MMP indicates the initiation of apoptosis.[25] Therefore, exposure to CTAB–AuNRs might damage the lysosomal membrane, which increases LMP (supported by AO staining in Fig. 5a and TEM images in Fig. 5b and c), and finally induced cell death. However, the other three kinds of AuNRs did not damage cell membrane and thus they did not change LMP (Fig. 5a), and MMP (Fig. 5d), and caused negligible effects on cell viability (Fig. 2a).

The interaction of CTAB–AuNRs with membrane systems including the cell membrane (serum-free system) and lysosomal membrane (complete medium system) seemed to be similar, due to possibly direct exposure of the CTAB surface to the membrane. The serum-free system is appropriate to study the nature of surface effects of nanomaterials on membrane structures, and it helps understand why CTAB–AuNRs are more

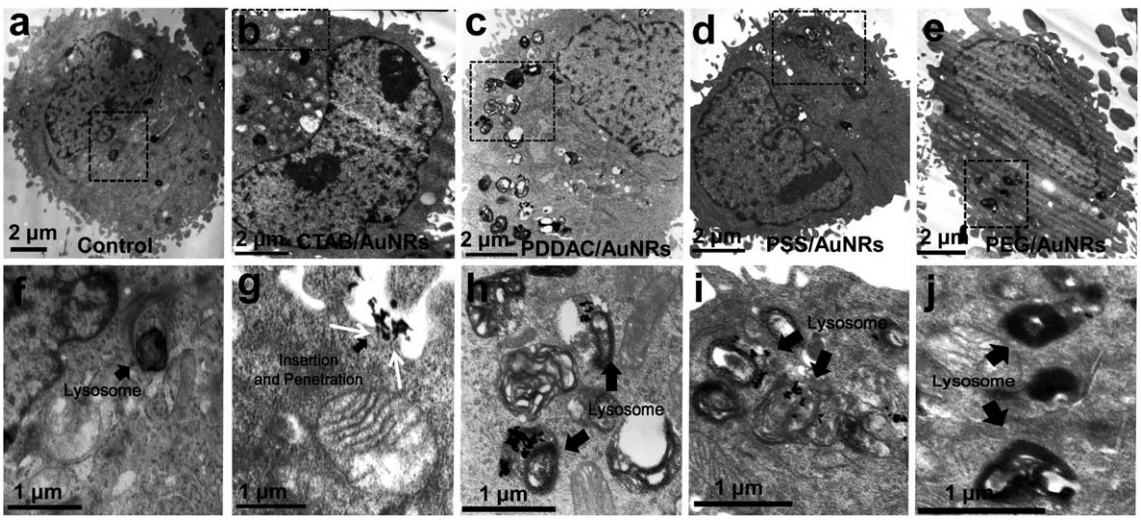

Fig. 4 TEM images of cytoplasm membranes and intracellular ultrastructures. In serum-free medium, untreated A549 cells (a and f); A549 cells exposed to 50 μM AuNRs with four kinds of surface coating, CTAB (b and g), PDDAC (c and h), PSS (d and i) and HS-PEG-COOH (e and j) for 12 h, respectively. The above figures (a–e) represent a whole cell image and their magnified images are shown below (f–j). In (g–j) the black arrowheads show lysosomes or AuNRs within lysosomes, while the white arrowheads indicate AuNRs inserted in the cell membrane.

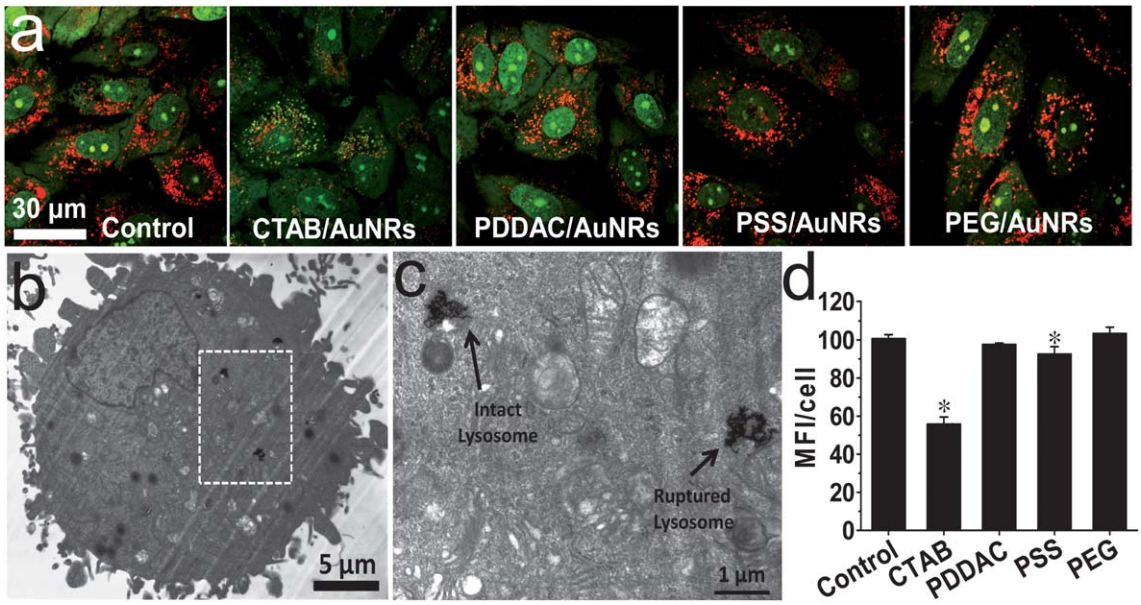

Fig. 5 The changes in lysosomal membrane integrity as determined by AO staining (a) and TEM images (b and c) and mitochondrial membrane potentials determined by mean fluorescence intensity (MFI) of intracellular Rh123 (d) when A549 cells were exposed to 50 μM AuNRs cultured in a complete cell culture medium, (b) represents a whole cell image and its magnified images are shown as (c) and the arrowheads point at the lysosomes containing AuNRs. * Represents significant effects of AuNRs on cells ($p < 0.05$). Results are reported as mean values and standard deviations, $N = 3$.

toxic than AuNRs with other surface coatings due to rupture of the lysosomal membrane structure.[15,16,22]

Interestingly, previous work has pointed out that surface charge is one major factor inducing nanoholes in membrane structures and was supported by atomic force microscopy or theory simulations.[27,28] However, in these studies supported lipid bilayers were used as the artificial membrane systems. They are quite different from actual lipid bilayer membranes in living systems like cells which can mediate membrane fluidity and balance in order to protect the cells from stimuli. Here, our study suggests that the interaction of nanomaterials with the membrane is complicated and a simple conclusion based on surface charge is improper. Both PDDAC and CTAB molecules have similar quaternary ammonium groups, which contribute to the positive charge on the surface of the AuNRs. With respect to quaternary ammonium functionalized nanoparticles, several groups gave different conclusions about the toxicity and possible nature of potential injury to the cell membrane. Quaternary ammonium-functionalized monolayer protected gold nanoparticles (AuNPs) had strong cytotoxicity, induced hemolysis and disrupted artificial vesicles composed of negative lipids, while carboxylate-substituted AuNPs did not show obvious toxicity. The authors proposed that positively charged AuNPs can bind to the membrane surface *via* electrostatic forces, which might disrupt the membrane and induce toxicity.[29] Another study reported that similar quaternary ammonium groups on AuNPs could produce membrane depolarization and increase the concentration of intracellular calcium ions, which finally resulted in increased apoptosis and inhibited cellular proliferation, depending on cell type.[30] However, in these studies the concentration of AuNPs, between 10 nM and 1 μM, was much higher than that of the AuNRs in our study (below 1 nM).[15,16,22] In such high concentration, strong electrostatic forces will probably induce significant effects on the structure and function of the cell membrane.

In our study, CTAB–AuNRs at only 70 pM (50 μM gold atom concentration) could show distinct surface effects. CTAB is a cationic surfactant, which assembles and forms a bilayer structure on the AuNRs during their synthesis. The bilayer has hydrophilic heads facing towards the aqueous environment and hydrophobic chains facing towards the nanorod core. The CTAB bilayer is stable in ion free systems and will be easily destabilized by increasing the ionic strength, which can be observed from the aggregates of AuNRs in the cell-free medium or lysosomes. Importantly, the CTAB bilayer shares a similar amphipathic structure to the lipid layer in the membrane but has opposite surface charges, which contributed to the injury of the membrane structure by CTAB–AuNRs. Proper strategies have been applied to explain why the CTAB surface is most toxic and how to reduce its toxicity. One common strategy is to coat AuNRs *via* layer by layer assembly using polyelectrolytes like PSS and PDDAC, which makes the AuNRs more stable and shields the toxic inner CTAB bilayer.[15,16] Another strategy is to fix the CTAB bilayer on the surface *via* polymerization or exchanging CTAB with 11-(acryloyloxy) undecyl trimethylammonium bromide (*p*-CTAB), which enhances the stability of the AuNRs and prevents the release of toxic CTAB from the surface improving biocompatibility.[31] The other option is to replace CTAB sufficiently with its thiolated analogue 16-mercaptohexadecyl trimethyl ammonium bromide (MTAB) on the AuNRs.[21] The MTAB thiol monolayer has a hydrophilic head facing towards the aqueous environment and a stable gold–thiol bond at the nanorod core. This replacement makes MTAB–AuNRs well dispersed in the solution, allows high cell uptake and

causes negligible toxicity even up to a 10 fold increase of the IC_{50} concentration of CTAB–AuNRs. The above strategies suggest that the toxic nature of CTAB–AuNRs originates from the surface adsorbed CTAB when they interact with the membrane structure of cells.

The surface chemistry of AuNRs includes multiple factors like surface charge, chemical nature, hydrophobic and hydrophilic properties, and so on. Previous work usually gave a general conclusion that surface chemistry mediates the cytotoxicity of AuNRs.[11,16] Herein, we have clearly demonstrated that the nature of the surface molecules especially their assembled structures, hydrophobic or hydrophilic properties probably play more crucial roles in determining cytotoxicity than surface charge alone. A positively charged CTAB bilayer on the AuNR surface is the dominant factor causing damage to the cell membrane and subsequent cell death. Further coating of polyelectrolyte multilayers such as PSS and PDDAC can efficiently reduce the cytotoxicity. In addition, previous work gave us a snapshot of the influences of surface molecules on organelles and subsequent cytotoxicity, however, it lacked more detailed evidence for interfacial interaction.[11,16] Surface analysis using ESEM can help obtain detailed information about the impairment of membrane structures, which can provide a basic explanation of how surface chemistry mediates cytotoxicity. Importantly, the present research expands our knowledge and focuses on the interfacial interaction between AuNRs and the membrane structure.

Conclusions

In conclusion, our results showed that the strong cytotoxicity of CTAB–AuNRs comes from the unique CTAB bilayer structure rather than the surface charge of the quaternary ammonium ions on the surface. Using ESEM and TEM, we observed that CTAB–AuNRs, rather than positively charged PDDAC–AuNRs, could insert and penetrate into cell membrane to form defects and then induce injury to the cell membrane in a serum-free system. The damage to the cell membrane caused by CTAB–AuNRs induced LDH release, decreased cell viability, and finally triggered cell death. The results describing the interaction of the CTAB surface and cell membrane can be used to understand why internalized CTAB–AuNRs could increase lysosomal membrane permeation, decrease the mitochondrial membrane potential, and finally result in cell death in complete cell culture medium. This study may help understanding of the toxic nature of AuNRs and guide design of the surface chemistry of AuNRs towards good compatibility for target therapy.

Experimental

Chemicals and biomaterials

Sodium borohydride ($NaBH_4$), hydrogen tetrachloroaurate(III) trihydrate ($HAuCl_4 \cdot 3H_2O$), cetyl trimethyl ammonium bromide (CTAB), silver nitrate ($AgNO_3$), sodium sulfate (Na_2SO_4) and L-ascorbic acid (AA) were purchased from Alfa Chemical (UK). Fetal bovine serum (FBS) was obtained from Gibco. Ultrapure Milli-Q water (18 MΩ cm, Millipore-Q) was used for all solution preparations. Acridine orange (AO), Rhodamine 123 and a live–dead Cell Assay Kit were obtained from Invitrogen. Low glucose Dulbecco's Modified Eagle's Medium (DMEM), penicillin, streptomycin and L-glutamine were purchased from Hyclone. Human lung carcinoma cell line (A549) was obtained from the American Type Culture Collection (ATCC).

CTAB-coated AuNRs

The seed-mediated growth method was employed to synthesize CTAB-capped AuNRs. At first, Au seeds were prepared by chemical reduction of $HAuCl_4$ with $NaBH_4$: 7.5 mL 0.1 M CTAB was mixed with 250 μL 10 mM $HAuCl_4$ and the volume was made up to 9.4 mL by adding water. Then, an ice-cold $NaBH_4$ aqueous solution (0.01 M) was added to the mixture to form seeds immediately. The seeds were used within 2–5 hours. The growth solution for AuNRs consisted of a mixture of 100 mL 0.1 M CTAB, 5 mL 0.01 M $HAuCl_4$, 1 mL 10 mM $AgNO_3$, 2 mL 0.5 M H_2SO_4 and 800 μL 0.1 M ascorbic acid. Growth was initiated by adding 240 μL seeds and stopped after 12 h by centrifuging twice at 9000 rpm for 7 min. The CTAB-capped AuNRs were dispersed in deionized water and the final concentration was adjusted to 2.5 mM.

Surface coating of AuNRs with polyelectrolytes and HS-PEG-COOH

The preparation of multilayer polyelectrolyte-coated AuNRs was achieved *via* a layer-by-layer assembly approach. The multilayer polyelectrolyte-coated AuNRs were synthesized by sequentially coating negatively charged PSS and positively charged PDDAC onto the as-synthesized CTAB-coated AuNRs. For the PSS coating, 12 mL AuNRs were centrifuged at 12 000 rpm for 10 min, and the precipitate was dispersed in 12 mL of 2 mg mL^{-1} PSS aqueous solution (containing 6 mM NaCl). Then the solution was stirred magnetically for 3 h. After that, it was centrifuged at 12 000 rpm for 10 min, and the precipitate was redispersed in water. For further coating with PDDAC, a similar procedure was applied to PSS-coated AuNRs. For the HS-PEG-COOH coating, as-synthesized AuNRs were washed twice and were then used to prepare 700 pM AuNR solutions by adding 700 mM carboxyl mercapto-PEG (M_w = 1000) to remove the surface CTAB molecules. The mixtures were sonicated overnight, and then centrifuged twice to separate the supernatant and PEG-coated AuNRs.

Characterization

For size and shape characterization, CTAB–AuNRs aqueous suspensions were dropped on carbon-coated copper grids and dried, and then observed by TEM (FEI Tecnai G2 F20 U-TWIN transmission electron microscope). The absorption spectra of 200 μM AuNRs (gold atom concentration) were obtained with a PerkinElmer UV-vis/near-infrared spectrophotometer (Lamdba 950). The zeta potentials were measured for 200 μM AuNRs in water. Triplicate samples for each group were determined by a zeta potential analyzer (Malvern Zetasizer Nano ZS).

The observation of cell morphology using an Environmental Scanning Electron Microscope (ESEM)

Cells were cultured on glass slices within Petri dishes for 24 h and exposed to AuNRs for 12 h. After fixation with 2.5% glutaraldehyde (v/v) in PBS for 40 min, cells were post-fixed with 1% osmic acid in PBS for 1 h and dehydrated gradually with a graded series of ethanol solutions and dried using a critical point drier. Cell samples on slices were placed on the specimen holder and imaged with the ESEM (Quanta 200 FEG, FEI Co.). Representative pictures were captured from at least eight randomly selected areas.

Cell imaging using a Transmission Electron Microscope (TEM)

Cells were cultured on Petri dishes and exposed to the AuNRs as described above. The cells were detached from the dishes with trypsin and collected as cell pellets. The pellets were then fixed and post-fixed as described above, dehydrated in a graded series of ethanol solutions, treated with propylene oxide, and embedded in Epon. Approximately 80 nm thick sections were cut into slices, placed on a carbon film supported by copper grids, stained with uranyl acetate and lead citrate and observed using a TEM (Hitachi) at 80 kV. Representative pictures were captured from at least eight randomly selected areas at magnifications of $\times$6000 and $\times$20 000, respectively.

Cell viability and LDH assay

About 5000 cells were seeded in 96 well plates for 24 h and exposed to 50 μM AuNRs and CTAB supernatant (isolated by centrifugation from CTAB–AuNRs in serum-free medium at 12 000 rpm for 10 min) for 12 h and 24 h, respectively. Cell viability was determined using a Cell Counting Kit-8 (CCK-8, Dojindo Laboratories in Japan). The absorbance was measured at 450 nm with a reference at 600 nm using an Infinite M200 microplate reader (Tecan, Durham, USA). With respect to the LDH assay, cells were exposed to 50 and 100 μM AuNRs and CTAB supernatant as mentioned above for 24 h. CytoTox-ONE™ Homogeneous Assay (Promega) was used to evaluate the released LDH in the culture medium using the fluorescence method, which was suitable to study the cytoplasmic membrane integrity. The CTAB supernatant was prepared in the serum free medium, which is derived from free CTAB in solution and partly desorbed CTAB from the AuNRs, which is used to understand whether the origin of the toxic effects is from surface properties or released molecules. The CTAB supernatant is employed in a series of experiments as below.

Live–Dead assay

LIVE/DEAD Viability/Cytotoxicity Kit (Molecular Probes) was used to distinguish live cells (stained with calcein AM, green fluorescence) from dead ones (stained with thidium homodimer, red fluorescence). Briefly, A549 cells were treated with 50 μM AuNRs or CTAB supernatant for 12 h. Then cells were stained with the kit and observed under a fluorescence microscope (Olympus $\times$60).

Assessment of lysosome membrane permeation (LMP)

Cells were seeded in 35 mm Petri-dishes for 24 h and rinsed twice with PBS. Cells were then incubated in a complete medium with 5 μg mL^{-1} AO and 10% FBS for 15 min. After 6 h of treatment with 50 μM AuNRs, the LMP of A549 cells was analyzed under a confocal microscope with excitation at 488 nm, and emission at 537 nm (green) and 615 nm (red) (Perkin Elmer Ultra View Vox system, USA).

Assessment of mitochondrial membrane potential (MMP) using Rhodamine 123

The MMP was assessed quantitatively by flow cytometry. Adhered cells were seeded in 6-well plate for 24 h. After washing with PBS three times, the cells were treated with 50 μM AuNRs in the complete medium for 24 h. Then, the cells were incubated in phenol red-free medium containing 5 μg mL^{-1} Rhodamine 123 for 30 min. After rinsing with PBS three times, the cells were digested, collected and measured by flow cytometry using the FL1 channel.

Statistical analysis

Results (mean and standard deviation) were analyzed for normal distribution (one-way or repeated measures ANOVA). Differences were considered statistically significant for $p < 0.05$.

Conflict of interest

The authors declare no competing financial interest.

Acknowledgements

This work was financially supported by the National Basic Research Program of China (2011CB933401, 2010CB934004 and 2012CB934000), the National Natural Science Foundation of China (11205166 and 31070854), International Science & Technology Cooperation Program of China (2013DFG32340), National Major Scientific Instruments Development Project (2011YQ03013406) and German Federal Ministry of Education and Research (BMBF 0315773A). We are very grateful to Prof. Dong Han and Ms Jiayi Xie from NCNST for the ESEM experiment, and Mr Jun Pan and Prof. Jingyuan Li from IHEP in Beijing for discussion.

Notes and references

1 E. C. Dreaden, A. M. Alkilany, X. Huang, C. J. Murphy and M. A. El-Sayed, *Chem. Soc. Rev.*, 2012, **41**, 2740–2779.
2 X. H. Huang, I. H. El-Sayed, W. Qian and M. A. El-Sayed, *J. Am. Chem. Soc.*, 2006, **128**, 2115–2120.
3 H. Wang, T. B. Huff, D. A. Zweifel, W. He, P. S. Low, A. Wei and J. X. Cheng, *Proc. Natl. Acad. Sci. U. S. A.*, 2005, **102**, 15752–15756.
4 J. Kneipp, H. Kneipp, M. McLaughlin, D. Brown and K. Kneipp, *Nano Lett.*, 2006, **6**, 2225–2231.
5 R. A. Sperling, P. R. Gil, F. Zhang, M. Zanella and W. J. Parak, *Chem. Soc. Rev.*, 2008, **37**, 1896–1908.

6 H. Chen, L. Shao, Q. Lia and J. Wang, *Chem. Soc. Rev.*, 2013, **42**, 2679–2724.
7 L. Dykman and N. Khlebtsov, *Chem. Soc. Rev.*, 2012, **41**, 2256–2282.
8 X. M. Jiang, L. M. Wang, J. Wang and C. Y. Chen, *Appl. Biochem. Biotechnol.*, 2012, **166**, 1533–1551.
9 Z. Zhang, L. Wang, J. Wang, X. Jiang, X. Li, Z. Hu, Y. Ji, X. Wu and C. Chen, *Adv. Mater.*, 2012, **24**, 1418–1423.
10 L. G. Xu, Y. Liu, Z. Y. Chen, W. Li, Y. Liu, L. M. Wang, Y. Liu, X. C. Wu, Y. L. Ji, Y. L. Zhao, L. Y. Ma, Y. M. Shao and C. Y. Chen, *Nano Lett.*, 2012, **12**, 2003–2012.
11 L. M. Wang, Y. Liu, W. Li, X. M. Jiang, Y. L. Ji, X. C. Wu, L. G. Xu, Y. Qiu, K. Zhao, T. T. Wei, Y. F. Li, Y. L. Zhao and C. Y. Chen, *Nano Lett.*, 2011, **11**, 772–780.
12 Y. Min, C.-Q. Mao, S. Chen, G. Ma, J. Wang and Y. Liu, *Angew. Chem., Int. Ed.*, 2012, **51**, 6742–6747.
13 Z. Xiao, C. Ji, J. Shi, E. M. Pridgen, J. Frieder, J. Wu and O. C. Farokhzad, *Angew. Chem., Int. Ed.*, 2012, **51**, 11853–11857.
14 B. D. Chithrani, A. A. Ghazani and W. C. W. Chan, *Nano Lett.*, 2006, **6**, 662–668.
15 T. S. Hauck, A. A. Ghazani and W. C. Chan, *Small*, 2008, **4**, 153–159.
16 Y. Qiu, Y. Liu, L. M. Wang, L. G. Xu, R. Bai, Y. L. Ji, X. C. Wu, Y. L. Zhao, Y. F. Li and C. Y. Chen, *Biomaterials*, 2010, **31**, 7606–7619.
17 T. Niidome, M. Yamagata, Y. Okamoto, Y. Akiyama, H. Takahashi, T. Kawano, Y. Katayama and Y. Niidome, *J. Controlled Release*, 2006, **114**, 343–347.
18 X. Huang, X. Peng, Y. Wang, Y. Wang, D. M. Shin, M. A. El-Sayed and S. Nie, *ACS Nano*, 2010, **4**, 5887–5896.
19 L. M. Wang, Y. F. Li, L. J. Zhou, Y. Liu, L. Meng, K. Zhang, X. C. Wu, L. L. Zhang, B. Li and C. Y. Chen, *Anal. Bioanal. Chem.*, 2010, **396**, 1105–1114.
20 B. Nikoobakht and M. A. El-Sayed, *Langmuir*, 2001, **17**, 6368–6374.
21 L. Vigderman, P. Manna and E. R. Zubarev, *Angew. Chem.*, 2012, **124**, 660–665.
22 A. M. Alkilany, P. K. Nagaria, C. R. Hexel, T. J. Shaw, C. J. Murphy and M. D. Wyatt, *Small*, 2009, **5**, 701–708.
23 E. Ito, K. W. Yip, D. Katz, S. B. Fonseca, D. W. Hedley, S. Chow, G. W. Xu, T. E. Wood, C. Bastianutto, A. D. Schimmer, S. O. Kelley and F. F. Liu, *Mol. Pharmacol.*, 2009, **76**, 969–983.
24 M. Z. Liu and P. Guyot-Sionnest, *J. Phys. Chem. B*, 2005, **109**, 22192–22200.
25 F. Lao, L. Chen, W. Li, C. Ge, Y. Qu, Q. Sun, Y. Zhao, D. Han and C. Chen, *ACS Nano*, 2009, **3**, 3358–3368.
26 W. Li, L. Zhao, T. T. Wei, Y. L. Zhao and C. Y. Chen, *Biomaterials*, 2011, **32**, 4030–4041.
27 P. R. Leroueil, S. A. Berry, K. Duthie, G. Han, V. M. Rotello, D. Q. McNerny, J. R. Baker, B. G. Orr and M. M. B. Holl, *Nano Lett.*, 2008, **8**, 420–424.
28 J. Lin, H. Zhang, Z. Chen and Y. Zheng, *ACS Nano*, 2010, **4**, 5421–5429.
29 C. M. Goodman, C. D. McCusker, T. Yilmaz and V. M. Rotello, *Bioconjugate Chem.*, 2004, **15**, 897–900.
30 R. R. Arvizo, O. R. Miranda, M. A. Thompson, C. M. Pabelick, R. Bhattacharya, J. D. Robertson, V. M. Rotello, Y. S. Prakash and P. Mukherjee, *Nano Lett.*, 2010, **10**, 2543–2548.
31 A. M. Alkilany, P. K. Nagaria, M. D. Wyatt and C. J. Murphy, *Langmuir*, 2010, **26**, 9328–9333.